Marine Ecology
June 2019, Volume 40, Issue 3, Pages e12541 (16p.)
https://doi.org/10.1111/maec.12541
https://archimer.ifremer.fr/doc/00493/60426/

Ecophysiological differences between vesicomyid species and metabolic capabilities of their symbionts influence distribution patterns of the deep- sea clams

Cruaud Perrine [1, 2, 3, *], Decker Carole [4], Olu Karine [4], Arnaud-Haond Sophie [4, 5], Papot Claire [4], Le Baut Jocelyn [4], Vigneron Adrien [1, 2, 3], Khripounoff Alexis [4], Gayet Nicolas [4], Cathalot Cecile [4], Caprais Jean-Claude [4], Pignet Patricia [1, 2, 3], Godfroy Anne [1, 2, 3], Cambon-bonavita Marie-anne [1, 2, 3]

[1] IFREMER, Laboratoire de Microbiologie des Environnements Extrêmes UMR6197, Technopôle Brest Iroise Plouzané, France
[2] Laboratoire de Microbiologie des Environnements Extrêmes Université de Bretagne Occidentale, UMR6197 Plouzané ,France
[3] CNRS, Laboratoire de Microbiologie des Environnements Extrêmes UMR6197, Technopôle Brest Iroise Plouzané ,France
[4] IFREMER, Centre Bretagne, Laboratoire Environnement Profond REM-EEP-LEP, Technopôle Brest Iroise Plouzané ,France
[5] MARBEC, Institut Français de Recherche pour L'Exploitation de la Mer Univ Montpellier, CNRS, IRD Sète ,France

* Corresponding author : Perrine Cruaud, email address : perrine.cruaud@gmail.com

Abstract :

This study provides an analysis of vesicomyid bivalve–symbiont community distribution across cold seep and hydrothermal vent areas in the Guaymas Basin (Gulf of California, Mexico). Using a combination of morphological and molecular approaches including fluorescent in situ hybridization (FISH), and electronic microscopy observations, vesicomyid clam species and their associated symbionts were characterized and results were analyzed in light of geochemical conditions and other on-site observations. A greater diversity of vesicomyids was found at cold seep areas, where three different species were present (Phreagena soyoae [syn. kilmeri], Archivesica gigas, and Calyptogena pacifica). In contrast, A. gigas was the only species sampled across the hydrothermal vent area. The same haplotype of A. gigas was found in both hydrothermal vent and cold seep areas, highlighting possible contemporary exchanges among neighboring vents and seeps. In either ecosystem, molecular characterization of the symbionts confirmed the specificity between symbionts and hosts and supported the hypothesis of a predominantly vertical transmission. In addition, patterns of clams could reflect potential niche preferences for each species. The occurrence of numerous traces of vesicomyid movements on sediments in the sites colonized by A. gigas seemed to indicate that this species might have a better ability to move. Furthermore, variation in gill sulfur content could reveal a higher plasticity and sulfur storage capacity in A. gigas. Thus, the distribution of vesicomyid species across the chemosynthetic areas of the Guaymas Basin could be explained by differences in biological traits of the vesicomyid species that would allow A. gigas to more easily exploit transient and punctual sources of available sulfide than P. soyoae.

Keywords : deep-sea ecosystems, Guaymas Basin, marine ecology, pliocardinae bivalve, sulfur storage, vesicomyid movements

1. Introduction

Deep-sea hydrothermal vents and cold seeps are submarine environments where reduced fluids emanate from the sea floor. They occur in a variety of geological settings throughout the global ocean and support complex food webs based on microbial chemoautotrophic primary production (Van Dover et al., 2002). In these environments, dense faunal assemblages dominated by Vesicomyidae clams, Mytilidae mussels, Alvinocarididae shrimps and Siboglinidae tubeworms, associated with bacterial symbionts, benefit from chemical energy of the fluid emission (Tunnicliffe, 1991; Sibuet and Olu, 1998; Dubilier et al., 2008).

In sulfide-rich environments such as cold seeps and hydrothermal vents, vesicomyid bivalves are often the main components of the megafaunal communities (Tunnicliffe, 1991; Bennett et al., 1994; Sibuet and Olu, 1998; Krylova and Sahling, 2010). These clams live partially buried in sediments or in small fissures of the oceanic crust (Arp et al., 1984). While vesicomyids (sub-family Pliocardiinae : Krylova and Sahling, 2010) exhibit reduced digestive tracts (Fiala-Médioni and Le Pennec, 1989), their gills are hypertrophied and host large numbers of chemoautotroph sulfur-oxidizing symbiotic bacteria enclosed in specific cells named bacteriocytes (Cavanaugh, 1983; Fiala-Médioni and Métivier, 1986; Fisher, 1990; Childress et al., 1991). Most of the vesicomyid's energy needs, for growth and metabolism, are supplied by these thiotrophic symbionts (Cavanaugh, 1983; Fiala-Médioni and Métivier, 1986). The symbionts can oxidize various sulfur compounds, such as sulfide, thiosulfate and elemental sulfur, to produce the energy used to fuel inorganic carbon fixation *via* the Calvin-Benson-Bassham cycle (Goffredi and Barry, 2002; Newton et al., 2008). In exchange of carbon substrates (Fisher et al., 1988; Stewart et al., 2005), the invertebrate host facilitates access to substrates required for symbiont metabolism. Indeed, the clam's vascularized foot penetrates sediments to capture buried sulfide, while siphons bring oxygen from seawater (Arp et al., 1984). There are strong arguments in favor of an obligatory symbiosis for both partners. Symbionts are mainly maternally transmitted *via* eggs (Endow and Ohta, 1990; Cary and Giovannoni, 1993), leading to a typical co-evolution pattern highlighted in several studies (Peek et al., 1998; Stewart, 2008). Vesicomyids are very diverse with more than 100 described species (Krylova and Sahling, 2010).

However, only a few species are known to be shared between different types of chemosynthesis-based ecosystems (Peek et al. 1997). Although several aspects of their physiology are becoming well characterized (Goffredi and Barry, 2002, Decker et al., 2014, 2017), the factors driving their spatial distribution patterns among and within ecosystems remain poorly understood (Krylova and Sahling, 2010; Watanabe et al., 2013).

The Guaymas Basin is an active seafloor-spreading area located in the center of the Gulf of California (27°N, 11.5°W) (Otero et al., 2003), where both active hydrothermal vents and hydrocarbon seeps are present within close proximity to each other and in the absence of physical barriers (Figure 1) (Simoneit et al., 1990; Otero et al., 2003; Vigneron et al., 2013, Cruaud et al., 2017). This Basin exhibits a very high rate of sedimentation (2.7 mm per year) and is overlain by 400-500 m of sediments (Simoneit et al., 1990). The high-temperature and hydrocarbon-rich hydrothermal vents are located in the Southern Trough and are very different from rock-hosted vent systems such as those of the Mid-Atlantic Ridge, since they are covered by a thick layer of hydrothermally altered sediments (Von Damm et al., 1985; Martens, 1990; Simoneit et al., 1990; Otero et al., 2003). Just 60 km away from the hydrothermal vent area, cold seeps are located at the transform fault that crops out along the continental slope on the Sonora Margin (Simoneit et al., 1990; Paull et al., 2007). These two types of ecosystems both release hydrocarbon- and sulfide-rich fluids, fueling dense colonies of chemosynthetic organisms (Portail et al. 2015, Simoneit et al., 1990; Teske et al., 2002; Vigneron et al., 2013). Previous studies showed that different species of Vesicomyidae occurred in the Guaymas Basin. At the Southern Trough hydrothermal vent area, *Archivesica gigas* Dall, 1895 (Krylova and Sahling, 2010) and the species complex *Calyptogena pacifica* Dall, 1891 / *Calyptogena lepta* Dall 1896 (Goffredi et al., 2003; Krylova and Sahling, 2010; Audzijonyte et al., 2012) were reported (Grassle, 1986; Peek et al., 1997; Ruelas-Inzunza et al., 2003; Soto, 2009). *A. gigas, C. pacifica* and *Phreagena soyoae* (syn. *kilmeri*) (Okutani, 1957) (Krylova and Sahling, 2010; Audzijonyte et al., 2012) were sampled at the Sonora cold seep area (Simoneit et al., 1990; Peek et al., 1997; Audzijonyte et al., 2012). However these studies were based on few discrete samples, and so far no relationship has

been described between the distribution of those bivalves and the conditions present within their habitats in cold seep and hydrothermal vent areas.

Here, we propose to analyze the distributions of symbiotic vesicomyids across three cold seep sites and one hydrothermal vent site located in the Guaymas Basin. Our main objectives were to characterize vesicomyid species and associated symbionts at each sampling site and to highlight factors that could potentially explain the distribution and environmental niche preferences of each vesicomyid species. To this end, morphological and molecular identification of vesicomyids was performed in parallel with molecular characterization of symbiont lineages and microscopic analyses of both host and symbionts. The results were analyzed in light of environmental characterization of habitats and sites.

105

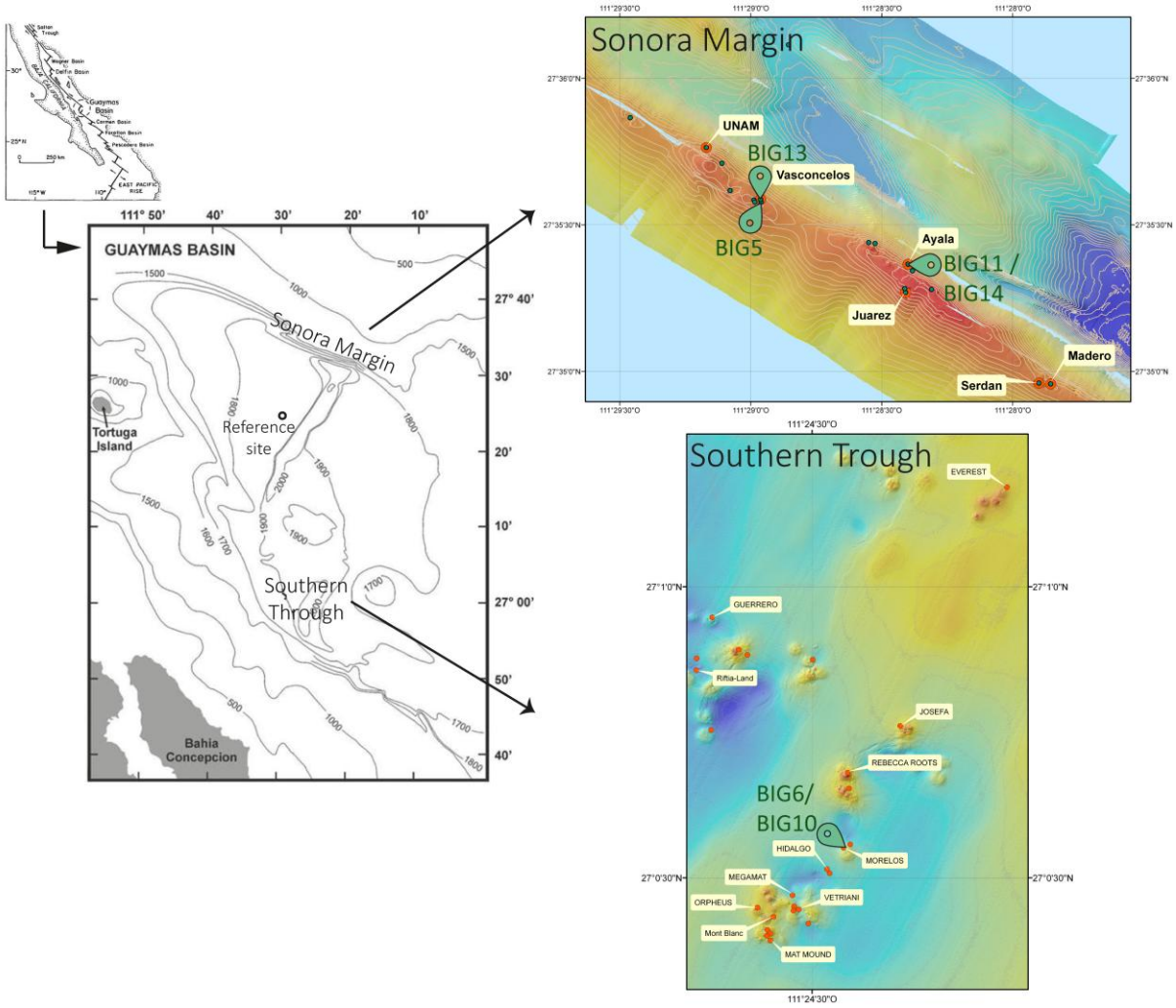

Figure 1 : Maps of the Guaymas Basin (adapted from Otero et al., 2003 and Simoneit et al, 1990) and location of sampling sites.

2. Materials and Methods

2.1. Studied sites and sampling

Vesicomyid clams were collected in June 2010 in the Guaymas Basin with the manned submersible Nautile during the "BIG" cruise. The sampling sites were selected following (1) an AUV-mounted multibeam survey (microbathymetry and backscatter) and (2) a concurrent tracking of acoustic anomalies in the water column by the RV *l'Atalante* multibeam revealing potential seep and vent sites (Ondréas et al., 2018), followed by (3) a visual exploration with the Nautile to check active sites on the seafloor. Among the surveyed and sampled sites, the *Ayala* (27°35.5796N; 111°28.9879W) and the *Vasconcelos* (27°35.5887N; 111°28.9663W) sites in cold seeps area (1 km apart) along the Sonora Margin and the *Morelos* site (27°00.5484N; 111°24.4219W) in hydrothermal vents area of the Southern Trough (60 km apart), showed the highest vesicomyid populations. The *Ayala* site is located at about 1,560 m depth and contains two markers (labeled BIG14 and BIG11, Figure 1, Table 1). The *Vasconcelos* site is located 1 km northwest from the *Ayala* site at about 1,570 m depth and is also marked in two locations (BIG13 and BIG5 about 10 m apart, Figure 1, Table 1). At the *Vasconcelos* site, visual features differed at markers BIG13 and BIG5, and those two locations were analyzed separately throughout the manuscript. Finally, the hydrothermal *Morelos* site was analyzed in Southern Trough, located 60 km apart at 2,007 m depth (BIG6 and BIG10 markers, Figure 1, Table 1). This site is located about 240 m north from the previously studied *MegaMat* site characterized by thick microbial mats at the sediment surface (Biddle et al., 2012; Cruaud et al., 2017 ; McKay et al., 2012). A reference site (27°25.4766N; 111°30.0660W) outside of the active area was also explored in order to compare geochemical features between active and inactive areas (Figure 1 and Table 1) (Cruaud et al., 2015, 2017).

A total of 208 vesicomyid clams were collected using nets or blade cores (see Portail et al., 2015; Olu et al., 2017). Among those, 77 vesicomyids were collected from the *Ayala* site, 56 from the *Vasconcelos* site (44 from BIG13 and 12 from BIG5) and 74 from the *Morelos* site (Table 1).

Site name		Location	Depth	Type of environment	Sediment texture	Sulfate	Sulfide	H_2S fluxes ($mmolH_2S.m^{-2}.d^{-1}$)	CH_4 fluxes ($nmolCH_4.m^{-2}.d^{-1}$)	Sampled species		
										P. soyoae (syn. *kilmeri*)	*C. pacifica*	*A. gigas*
Ayala	BIG14	27°35.5796N; 111°28.9879W	1560 m	seep	granular	Constant (28 mM)	Not detected	0	0.15	62 / 77 (81%)	10 / 77 (13%)	5 / 77 (6%)
Vasconcelos	BIG13	27°35.5887N; 111°28.9663W	1570 m	seep	soft and liquid	Constant (28 mM)	Not detected	0	0	1 / 44 (2%)	-	43 / 44 (98%)
	BIG 5	27°35.5780N; 111°28.9555W	1575 m	seep	soft and carbonate rich	Decrease with depth (4.7 mM at 19 cmbsf)	Increase with detph after 4 cmbsf (11 mM at 15 cmbsf)	162.2	19.2	9 / 12 (75%)	3 / 12 (25%)	-
Morelos	BIG 6	27°00.5484N; 111°24.4219W	2007 m	vent	soft and liquid	Decrease with depth after 5 cmbsf (13.5 mM at 15 cmbsf)	Increase with detph after 5 cmbsf (10 mM at 15 cmbsf)	99.9 ± 30.5	1.0 ± 0.2	-	-	74 / 74 (100%)
Reference		27°25.4766N; 111°30.0660W	1850 m	reference	granular	Constant (28 mM)	Not detected	-	-	-	-	-

Table 1 : Overview of some site features: location, depth, type of environment, main chemical features (lowest sulfate and highest sulfide porewater concentrations, based on push core measurements) and number of vesicomyids of each species sampled/total number of vesicomyids sampled.

Upon recovery, clams were washed with 0.2 µm filtered seawater and morphologically identified on board. Parts of gills and adductor muscles were frozen in liquid nitrogen and stored in the lab at -80°C for molecular characterization of bivalves and symbionts, and estimation of sulfur contents. The anterior region of the gills was fixed for fluorescence *in situ* hybridization analyses (FISH) as previously described (Duperron et al., 2005).

Temperature measurements were performed in surface sediments using an independent thermal lance T-Rov (NKE Electronics, France) at cold seep habitats or using the temperature sensor of the submersible at hydrothermal vents. Sediment push core samples (between 8 and 20 cm length) were also collected at each habitat for analyses of sediment porewaters as described in Cruaud et al., 2015 (one or two cores for each site). Porewaters were extracted using RHYZON samplers on push core sediments and kept in the dark in a cold room (4°C). Both sediment and water samples were processed on board for chemical analyses within 4 hours of recovery.

2.2. Water and porewater analyses

For measurements of total sulfide and methane concentrations, porewater samples were transferred into N_2-flushed vials and fixed for onshore analyses with saturated $ZnCl_2$ (1:1 $vol.vol^{-1}$) and $HgCl_2$ (20 µL) respectively. For sulfates, samples were acidified with 65% HNO_3 (1:1000 $vol.vol^{-1}$) and stored in plastic vials. Sulfate (SO_4^{-2}) and total sulfide (H_2S) concentrations were measured by ion exchange chromatography (Lazar et al., 2012) and colorimetry (Fonselius et al., 2007), respectively. Methane was analyzed by gas chromatography coupled with a headspace system (GC-HSS) (Sarradin and Caprais, 1996).

Diffusive fluxes of methane and sulfide were determined according to Fick's first law of diffusion :

$$J_{(species)} = -\emptyset \times D_{sed} \times \frac{\partial_C}{\partial_Z} \quad (1)$$

where $J_{(species)}$ is the diffusive flux of the dissolved species, $\varnothing$ represents sediment porosity, D_{sed} is the sediment diffusion coefficient in $cm^2.d^{-1}$, and $\frac{\partial_C}{\partial_Z}$ is the vertical concentration gradient of the dissolved species in $mol.m^{-4}$. Porosity was determined from the weight loss upon drying at 60°C until complete dryness of sediment core segments of known weight and volume. D_{sed} was calculated for ambient bottom water temperature and salinity and corrected for tortuosity using the Iversen & Jorgensen formulation for muds (Iversen and Jørgensen, 1993; Boudreau, 1996). Concentration gradients of sulfide and methane were determined from the measured porewater profiles obtained for each individual habitats.

2.3. DNA extraction

Among the 208 vesicomyid clams collected, 119 were used for molecular species identification (43 from the *Ayala* site, 34 from the *Vasconcelos* site and 42 from the *Morelos* site). For vesicomyid identification, total DNA was extracted from a piece of adductor muscle following the protocol by Doyle (1987).

Symbiont characterization was performed for 12 vesicomyid clams with 2 specimens per identified vesicomyid species for each sampling site. For this purpose, total DNA was extracted from gill samples using a CTAB extraction method (Zhou et al., 1996). Total DNA was purified using the Wizard® DNA Clean-Up System (Promega, USA). All DNA was stored at -20°C until used for PCR.

2.4. PCR amplification and sequencing for vesicomyid identification

The mitochondrial cytochrome c oxidase I (*COI*) standard barcode fragment was amplified using universal (LCO1490 and HCO2198 (Folmer et al., 1994)) and vesicomyid-specific (VesLCO and VesHCO (Peek et al., 1997)) primers (Table S1). The PCR reaction mix (50 µL) included: 1X Taq

DNA polymerase buffer (Promega, USA), 2.5 mM of $MgCl_2$, 0.20 mM of dNTPs, 0.6 mM of each primer, 0.5 U of Taq DNA polymerase (Promega, USA) and 5 µl of purified DNA. The PCR program involved an initial denaturation step at 94°C for 90 s, followed by 35 cycles of incubation at 94°C for 30 s, 45°C for 60 s, 72°C for 75 s and a final extension at 72°C for 10 min. PCR products were sent to GATC Biotech (Constance, Germany) for sequencing.

Sequences were processed using Geneious software (v.4.6. created by Biomatters. Available from http://www.geneious.com/). After cleaning of sequences or portions containing too many uncertainties, both strands for each overlapping fragment were assembled. Alignment was performed using MAFFT 6.903 (Katoh et al., 2005) and translated to amino acids to detect frameshift mutations and premature stop codons. Divergent haplotypes were deposited in GenBank under accession numbers KF953548-KF953666. BLAST was also performed through the dedicated Geneious plugin in order to ascertain molecular species identity (Altschul et al., 1990). COI sequences from close relatives were uploaded and included in phylogenetic analyses.

2.5. PCR amplification and sequencing for symbiont characterization

According to the results of vesicomyid identifications, 2 specimens per vesicomyid species from each site were used for symbiont characterization. Three different genes were amplified, cloned and sequenced : the 16S rRNA gene and two functional genes, adenosine-5'-phosphosulfate (APS) reductase (*aprA*) (Meyer and Kuever, 2007) and form II of the ribulose-1, 5- biphosphate (RuBP) carboxylase/oxygenase (*cbbM*)(Kato et al., 2012) (Table S1).

PCR amplifications were performed in triplicate using a GeneAmp® PCR System 9700 (Applied Biosystems, Forster City, CA) under the following conditions : 5 min at 95°C, then 30 cycles including 30 s at 95°C, 1 min 30 at the annealing temperature (Table S1) and 2 min at 72°C and a final step of 6 min at 72°C. The PCR reaction mix (25 µL) was composed of 1X Colorless GoTaq® Flexi Buffer (Promega, USA), 2 mM of $MgCl_2$ (Promega, USA), 0.2 µM of each primer (Eurogentec, Liège, Belgium), 0.4 mM of dNTP mix, 2.5U of GoTaq polymerase (Promega, USA) and 1 µL purified DNA template. PCR products were pooled and purified on TAE agarose gel (1.2%) using

PCR clean-up Gel extraction Nucleospin® Gel and PCR Clean-up kit (Macherey-Nagel, Düren, Germany). Purified PCR products were cloned using the TOPO®XL PCR Cloning Kit (Invitrogen, Life technologies, CA, USA) according to the manufacturer's instructions.

Amplicons were sequenced using ABI3730xl Genetic Analyzer (Applied Biosystems, Foster City, CA, USA) using M13 universal primers by GATC Biotech (Constance, Germany). A total of 248 amplicons were obtained for the 16S rRNA gene (120 clones for *P. soyoae*, 64 for *A. gigas* and 64 for *C. pacifica*), 96 for the *cbbM* gene (32 clones for each vesicomyid species) and 66 for the *aprA* gene (22 clones for each vesicomyid species).

We used Bioedit v.7.1 (Ibis Biosciences, Carlsbad, CA, USA) to remove vector and primer sequences. Alignments were performed using MAFFT 6.903 (Katoh et al., 2005) and protein-coding genes were translated to amino acids to detect frameshift mutations and premature stop codons. Divergent sequences for each gene were deposited in European Molecular Biology Laboratory (EMBL) nucleotide sequence database under accession numbers HG513073 - HG513078 for 16S, HG513079 – HG513084 for *aprA* and HG513085 – HG513090 for *cbbM*. Sequences were compared to the GenBank, EMBL and DDBJ databases using the NCBI Blast search program (Altschul et al., 1990). Several Blast hits from close relatives were downloaded and included in phylogenetic analyses.

2.6. Phylogenetic analyses

Phylogenetic trees from each individual gene were generated using distance (Neighbor-joining) and maximum likelihood (ML) methods. Pairwise nucleotide sequence divergences were calculated using a Kimura-2-parameter model of substitution (Kimura, 1980) for 16S rRNA and functional genes. Neighbor-joining trees (Saitou and Nei, 1987) were reconstructed using MEGA 4.0.2 (Tamura et al., 2007). Topological robustness was assessed by bootstrap procedures using 1,000 replicates (Felsenstein, 1985). ML analyses were performed with MPI-parallelized RAxML 7.2.8 (Stamatakis, 2006), using a GTR model with among site rate variation modeled by a discrete gamma approximation with four categories. GTRCAT approximation of models was used for ML bootstrapping (1,000 replicates). ML analyses were conducted on the CIPRES Science Gateway (Miller et al., 2010).

2.7. Microscopy

In situ hybridization analyses were performed as previously described (Durand et al., 2009), on 18 gill samples stored for FISH experiments. Universal probe Eub338 (Amann et al., 1990) and newly designed specific probes were used. Three different 16S rRNA probes were designed according to our 16S rRNA clone sequences, one for each species (Table S1). A negative control without any probe was used for each condition and host species. Several formamide concentrations (0, 20, 30, 35, 40, 45, 50, 60, 70 and 80%) were tested. A concentration of 35% formamide in hybridization buffer was chosen for best hybridization and specificity. Observations were performed with a Zeiss Imager Z2 microscope (Zeiss, Göttingen, Germany) and with an Axio Zoom V16 (Zeiss, Göttigen, Germany) both equipped with the slider module ApoTome (Zeiss), the Colibri light technology (Zeiss) and using an AxioCam MRm camera (Zeiss). Epifluorescence acquisitions were treated using the AxioVision or ZEN softwares (Zeiss).

The samples fixed for FISH were also used for binocular microscopy observations and for scanning electron microscopy (SEM). Samples for binocular microscopy observations were cut with a razor blade into 1 mm slices. Observations were performed using an Olympus SZX16 (Olympus, Japan) and visible light acquisitions were performed with a Digital Color Camera Model GO-3-CLR-10 (QImaging®, Canada) and treated using QCapture Pro 6.0 software (QImaging®, Canada).

Afterwards, samples for SEM were dehydrated by ethanol series and desiccated with hexamethyldisilazane (Sigma) for 45 min and 1 h 30 in a critical-point dryer CPD 300 (Leica, Germany). Further samples were metalized with gold and palladium (60/40) using a high resolution Sputter Coater (Quorum Technologies, Guelph, Canada). SEM observations and imaging were performed using a FEI Quanta 200 MK2 microscope (FEI, Oregon, USA) and microanalyses of sulfur granules were performed with EDX spectrometer (Oxford instruments, Abingdon, UK).

2.8. Measurement of gill sulfur contents

Sulfur concentrations were measured on five *P. soyoae* and five *A. gigas* gill samples per site. *C. pacifica* could not be studied due to the lack of sample. Gills were lyophilized and then grinded to

ensure homogenized samples. Samples were stored at room temperature in a desiccator until analysis. The determinations of sulfur contents in gills were performed using a CS125 Carbon/Sulfur Determinator (LEICO Corporation, Michigan, USA) (% sulfur *versus* dry mass). Sulfur contents between host species were compared and statistical analyses were performed using Kruskal-Wallis non-parametric test (Kruskal and Wallis, 1952). A Mann-Whitney-Wilcoxon test (Wilcoxon, 1945; Mann and Whitney, 1947) was used to compare specific differences among groups when Kruskal-Wallis indicated a significant difference. Data were analyzed using the R software (R Development Core Team, 2011).

3. Results

3.1. Site description

The *Ayala* site was characterized by soft but granular sediments and was covered by many small, densely populated vesicomyid aggregates scattered on an area of about 15 by 20 meters (Figure 2A). The bivalves had 2/3 or more of their shell outside the sediment. In contrast, vesicomyid beds distributed around microbial mats in the *Vasconcelos* site lived more deeply buried, with half or less of their shell above sediments that were fine and seemed softer than *Ayala* sediments (Figure 2B and 2C). Moreover, the two areas where the markers BIG13 and BIG5 were located at the *Vasconcelos* site clearly exhibited different visual features. While vesicomyids formed dense aggregates at BIG5 area (Figure 2C), they were more sparsely distributed at BIG13 (Figure 2B). Many V-shaped trails were observed at BIG13, probably indicating clam locomotion (Figure 2B) (Rosman et al., 1987; MacDonald et al., 1990), while no trail was observed at BIG5 (Figure 2C). Hereafter, BIG5 and BIG13 are treated separately. Finally, the hydrothermal *Morelos* site was characterized by a large sedimentary area covered by a thin white layer, probably corresponding to a microbial mat. A small crack emitting shimmering water was observed at the center of the patch suggesting hydrothermal fluid percolation. The periphery of this white area resembled the *Vasconcelos* BIG13 site since it

harbored sparse and mostly buried vesicomyids and many trails on sediments suggesting soft sediment and clam locomotion (Figure 2D).

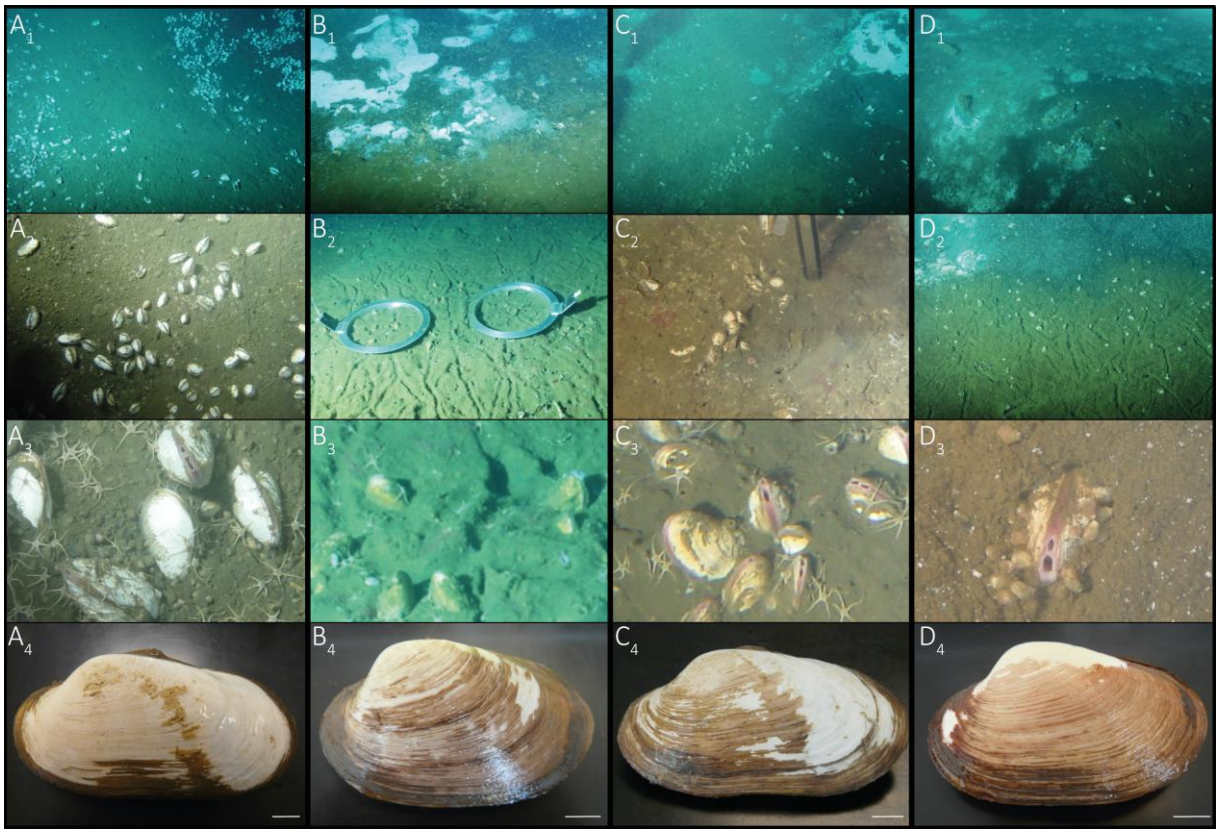

Figure 2 : Pictures of sampling sites : *Ayala* (A_{1-3}), *Vasconcelos BIG13* (B_{1-3}), *Vasconcelos BIG5*(C_{1-3}) and *Morelos* (D_{1-3}), and dominant vesicomyid species (A_4, B_4, C_4 and D_4). Scale bar = 1 cm. (A_4) and (C_4) *P. soyoae.* (B_4) and (D_4) *A. gigas.*

Measured temperatures were nearly identical (3°C) at the sediment surface around vesicomyids at each studied site. Temperatures were constant with depth at cold seep sites but increased from 3°C to 9.8°C at 30 cm below the seafloor (cmbsf) at the hydrothermal Morelos site.

3.2. Geochemical measurements

In sediments from the reference site, neither H_2S nor CH_4 was detected and the SO_4^{2-} profile showed constant values (around 27 $mmol.L^{-1}$ down to 17 cmbsf, data no shown).

The *Ayala* and *Vasconcelos* BIG13 sediments displayed similar porewater contents with constant SO_4^{2-} concentrations and no H_2S detected throughout the entire sediment core (0 to 10 cmsbsf) (Figure 3A and B). In *Vasconcelos* BIG13 sediments, very low concentrations of CH_4 were detected throughout the entire core and hence no associated flux was calculated. In *Ayala* sediments, CH_4 concentrations increased slightly from 0.6 µM at 3 cmsbf up to 13 µM at 8 cmbsf (Figure 3A). Upward diffusive CH_4 flux at 3 cm depth was calculated for the *Ayala* site to be 0.15 $nmol.m^{-2}.d^{-1}$ (n=1).

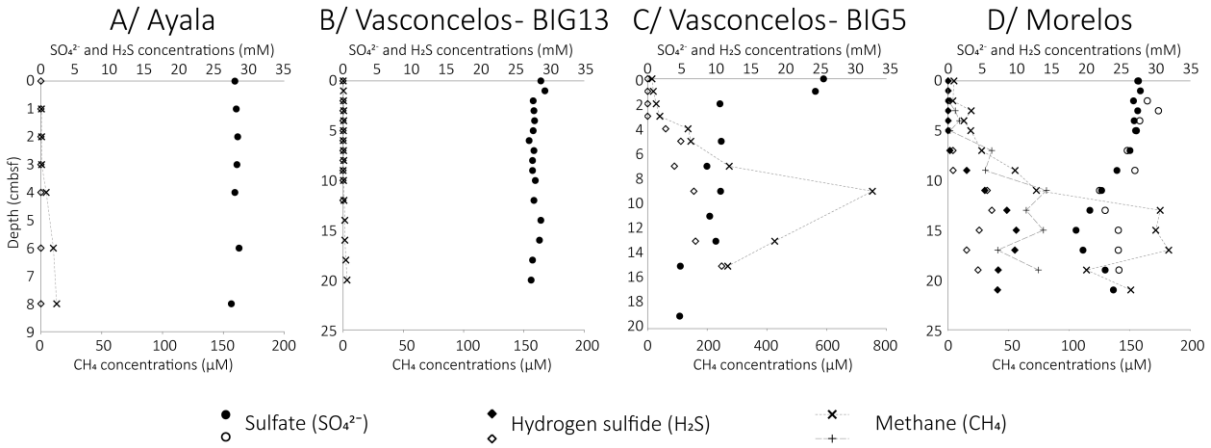

Figure 3 : Geochemical profiles of dissolved sulfide (diamond), sulfate (circle) and methane (cross) concentrations with depth in porewater sediments. Sediment cores were from (A) *Ayala*, (B) *Vasconcelos BIG13*, (C) *Vasconcelos BIG5* and (D) *Morelos* sites. Data on two core samples are represented for the *Morelos* site : CT5 (white circles, white diamonds and addition signs) and CT1 (black circles, black diamonds and cross).

In contrast, porewater data obtained at the *Vasconcelos* BIG5 site showed a sharp gradient in SO_4^{2-}, H_2S and CH_4 concentrations (Figure 3C). SO_4^{2-} concentrations decreased from 26 mM at the water/sediment interface to 4.7 mM at 19 cmbsf, while H_2S and CH_4 concentrations increased steeply reaching 11 mM at 15 cmbsf and 750 µM at 9 cmbsf respectively (Figure 3C). Associated upward fluxes were 162.2 mmol $H_2S.m^{-2}.d^{-1}$ and 19.3 nmol $CH_4.m^{-2}.d^{-1}$.

Porewater data obtained for the hydrothermal site (*Morelos* site) showed sulfate concentrations decreasing in the first 11 cmbsf, before increasing back to 24 mM at 21 cmbsf (Figure 3D). No sulfide was detected in the sediment above 5 cmsbf. Then, sulfide concentrations increased up to 10 mM at 15 cmbsf, leading to steep concentration gradients of sulfide. Methane concentrations increased steeply

up to 180 µM at 17 cmbsf. Methane and sulfide diffusive fluxes were estimated to be respectively 1.0 ± 0.2 nmol $CH_4.m^{-2}.d^{-1}$ and 99.9 ± 30.5 mmol $H_2S.m^{-2}.d^{-1}$ (n=2).

3.3. Vesicomyid species identification, distribution and behaviour

To the exception of the smallest specimens (about 5%) that could not be accurately identified through morphology, molecular and morphological approaches delivered congruent taxonomic identifications leading to the recognition of three distinct vesicomyid species (Table 1): *Phreagena soyoae*, *Calyptogena pacifica* and *Archivesica gigas*. With the exception of *C. pacifica* (intra-specific COI divergence = 0.2%), no intraspecific diversity was detected (Figure 4) as all specimens shared the same haplotype on 483 bp. Neighbor-joining and maximum likelihood trees obtained from our dataset and supplemented with databank sequences were similar (Figure 4). All our sequences strongly clustered with Genbank sequences obtained from conspecific individuals, which confirmed our identifications.

Species distribution varied among sites. At the Sonora Margin, the three vesicomyid species were sampled with a dominance of *P. soyoae* at *Ayala* (79% of bivalve sampled) and *Vasconcelos* BIG5 seep sites (75%). At both sites, vesicomyids appeared slightly buried in the sediments (Figure 2A and C). *A. gigas* was rare at the *Ayala* site (8% of the bivalves sampled) whereas it was the dominant species at the *Vasconcelos* BIG13 seep site (98%) (Table 1) where vesicomyids appeared almost entirely buried into sediments, most of them having only their siphons out (Figure 2D). *C. pacifica* was sampled at the *Ayala* and the *Vasconcelos* BIG5 seep sites (13% and 25% respectively). *A. gigas* was the only species sampled at the *Morelos* vent site (Southern Trough) where vesicomyids also appeared almost entirely buried into sediments (Figure 2D).

3.4. Symbiont characterization

Symbionts associated with each vesicomyid species were characterized using molecular analyses of i) 16S rRNA gene, ii) *aprA* gene encoding for a key enzyme catalyzing sulfide oxidation (APS reductase), and iii) *cbbM* gene encoding for a key enzyme in carbon fixation through the Calvin cycle (RuBisCO).

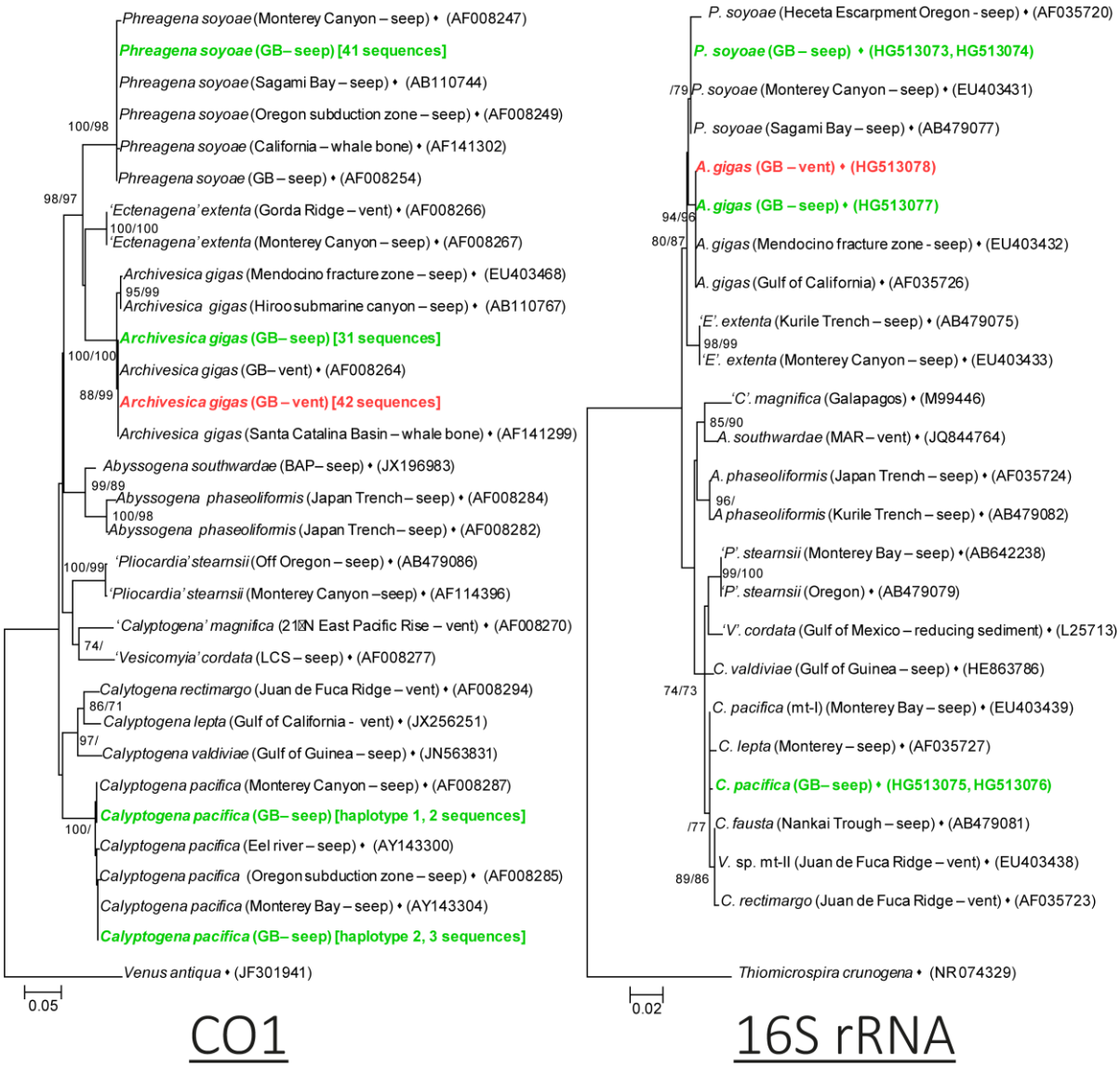

Figure 4 : Neighbor-Joining (NJ) phylogenic trees based on i) mitochondrial cytochrome c oxidase I (*COI*) sequences from vesicomyids and ii) 16S rRNA sequences from bacterial symbionts. For each data set, the maximum likelihood (ML) topologies were similar. Bootstrap supports (> 70) obtained for NJ / ML analyses are reported at nodes (1,000 replicates). Sequences from this study are highlighted in bold green for cold seep areas and bold red for hydrothermal vent area. Abbreviations : GB Guaymas Basin, BAP Barbados Accretionary Prism, LCS Louisiana Continental Slope, MAR Mid-Atlantic Ridge.

Topologies of neighbor-joining and maximum likelihood trees obtained for the supplemented 16S rRNA dataset were similar (Figure 4). Each host species harbored only one specific symbiont belonging to the *Gammaproteobacteria* subdivision (Figure 4).

AprA and *cbbM* partial sequences were translated into amino acids and encoded putative functional proteins (single ORF). Unfortunately, available sequences on Genbank were too scarce to construct larger phylogenetic trees. Phylogenetic analyses (ML and NJ) highlighted three different groups of closely related sequences corresponding to the three previously identified groups for hosts and symbionts. No difference was found between sequences from vents and seeps for *A. gigas*.

3.5. Morphological analysis and microscopy

In order to study symbiont localization in gills and to confirm specificity between symbiont and host, we combined binocular microscopy, SEM and FISH approaches.

In each observed gill, the frontal extremity of filaments, where ciliated cells were detected (Figure 5A, 6A, B, C, and E), could be distinguished by the thicker, abfrontal end where bacteriocytes containing symbionts were observed (Figure 5A, 6A, B, C and D). FISH observations showed that all cells in bacteriocytes hybridized with the universal probe. The *C. pacifica* symbiont probe hybridized only within *C. pacifica* gill cells that also labeled with the universal probe, but never in gill cells of any other vesicomyid species (Figure 5C), confirming the presence of a single symbiont. Unfortunately, 16S rRNA sequences from *P. soyoae* and *A. gigas* symbionts were too similar to result in specific hybridization, regardless of the formamide concentration used, and even using of the other probe as a competitor. However these two probes hybridized only in *P. soyoae* and *A. gigas* gill cells that also labeled with the universal probe, but never in gill cells of *C. pacifica*. This indicated closer similarity of *P. soyoae* and *A. gigas* symbionts, as shown in the tree (Figure 4).

Binocular microscope observations of dissected gills showed multiple white minerals, exclusively observed within the bacteriocyte zone (Figures 5A, 6A, B, C, D and S1A). They were not visible on SEM surface views and seemed to be embedded into gill tissue. Minerals were isolated and

357 then analyzed with SEM and EDX (Figure S1). EDX microanalyses on various backgrounds
358 (aluminum, copper) confirmed that they were sulfur particles (Figure S1 C, D, E, F).

359 *3.6. Measurement of gill sulfur contents:*

360 Gill sulfur contents were measured *versus* dry mass in the dominant species from each site. The
361 gill sulfur contents include all the non-volatile sulfur forms (sulfate, sulfite, elemental sulfur…). Sulfur
362 contents of *A. gigas* gills were significantly higher than in *P. soyoae* gills (16.14% and 11.27% in
363 average, respectively, p-value < 0.05). Detailed results are presented in Figure 7.

364

365

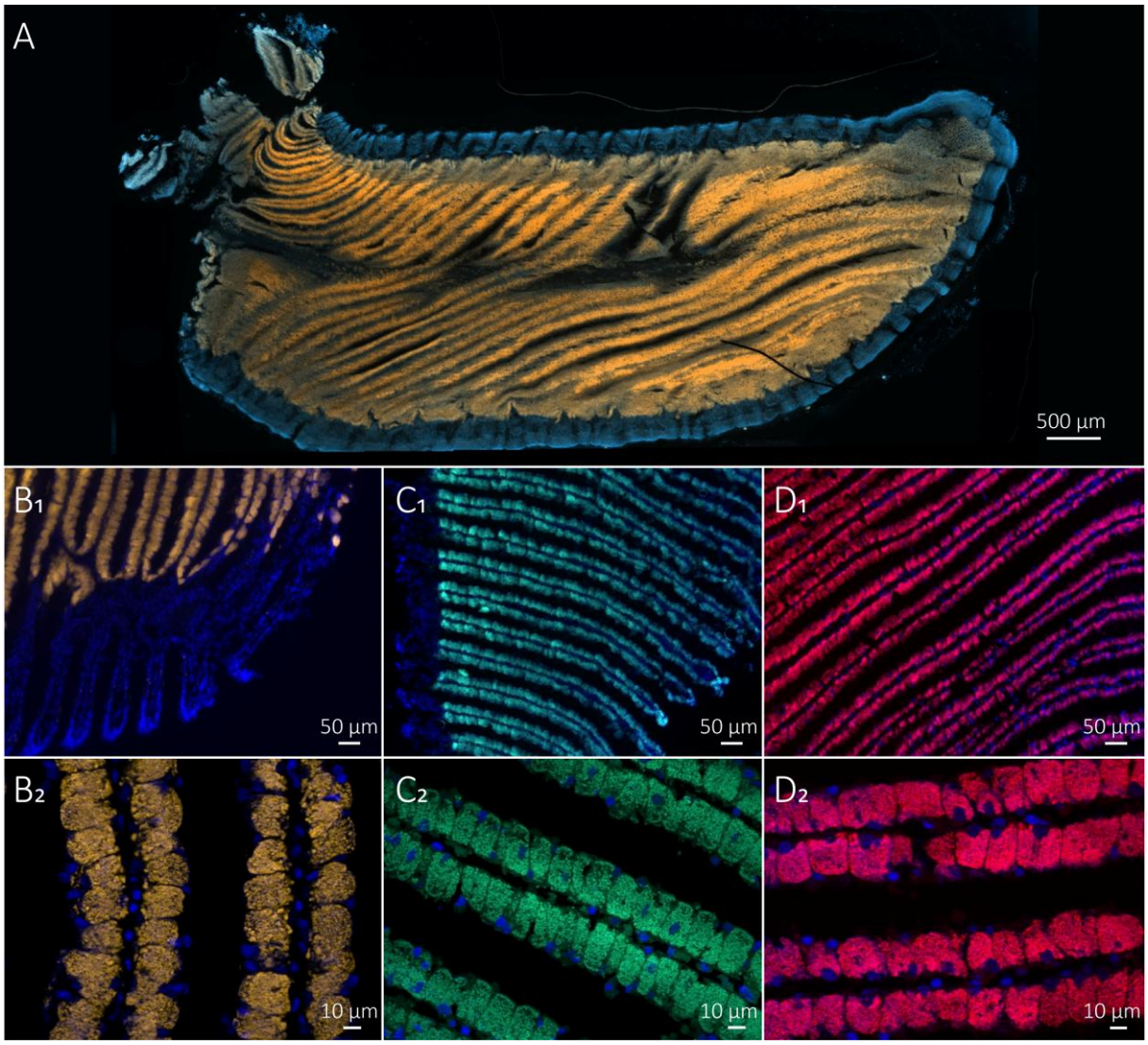

Figure 5 : Fluorescence *in situ* hybridization (FISH) images of symbiotic bacteria on transverse sections of vesicomyid gills at different magnifications. (A) *P. soyoae* gill, with symbionts hybridized with bacterial universal probe (in orange) in the abfrontal bacteriocyte zone and DAPI-stained frontal ciliated cells (in blue) at the periphery. Scale bar = 500 µm. ($B_{1\text{-}2}$), ($C_{1\text{-}2}$) and ($D_{1\text{-}2}$) Gill sections at larger magnification with symbionts hybridized with specific probe, *P. soyoae* ($B_{1\text{-}2}$), *C. pacifica* ($C_{1\text{-}2}$) and *A. gigas* ($D_{1\text{-}2}$). Transitions between frontal, ciliated region of gill filaments (in blue) and bacteriocyte zone (in orange and green) are presented on (B_1) and (C_1). (B_1), (C_1) and (D_1) Scale bars = 50 µm. (B_2), (C_2) and (D_2) Scale bars = 10 µm.

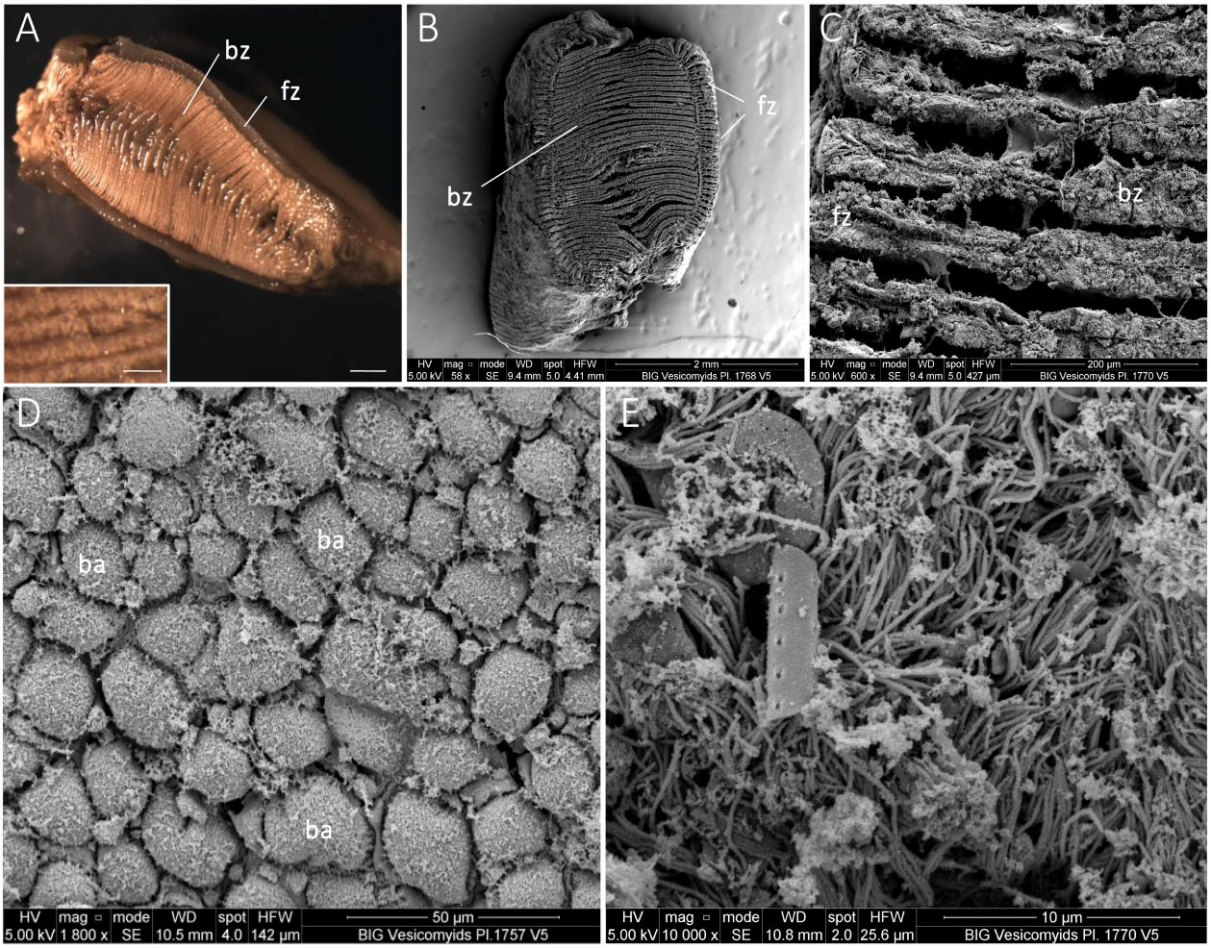

Figure 6 : (A) Image of a transverse section of gill fixed for FISH (binocular microscope), with inset showing higher magnification of the bacteriocyte zone, with "white minerals". Scale bars = 1 mm and 0.1 mm. (B), (C), (D) and (E) SEM views of gill sections. (B) Gill section at low magnification. (C) View of the gill filaments with ciliated cells on the left and bacteriocytes on the right. (D) View of bacteriocytes. (E) View of cilia in the frontal zone. (A), (B), (C), (D) and (E) *A. gigas.* fz, frontal ciliated zone ; bz, bacteriocyte zone ; ba, bacteriocyte.

SAMPLE	IDENTIFICATION	SITE	SULFUR (%)
1A	*P. soyoae*	Ayala	13.5
1B	*P. soyoae*	Ayala	7.0
1C	*P. soyoae*	Ayala	9.4
1D	*P. soyoae*	Ayala	12.0
1E	*P. soyoae*	Ayala	8.6
2A	*A. gigas*	Vasconcelos BIG13	17.3
2B	*A. gigas*	Vasconcelos BIG13	21.4
2C	*A. gigas*	Vasconcelos BIG13	18.1
2D	*A. gigas*	Vasconcelos BIG13	15.8
2E	*A. gigas*	Vasconcelos BIG13	24.6
3A	*P. soyoae*	Vasconcelos BIG5	17.0
3B	*P. soyoae*	Vasconcelos BIG5	10.0
3C	*P. soyoae*	Vasconcelos BIG5	8.7
3D	*P. soyoae*	Vasconcelos BIG5	15.2
4A	*A. gigas*	Morelos	8.5
4B	*A. gigas*	Morelos	21.7
4C	*A. gigas*	Morelos	14.5
4D	*A. gigas*	Morelos	9.6
4E	*A. gigas*	Morelos	11.0
4F	*A. gigas*	Morelos	15.0

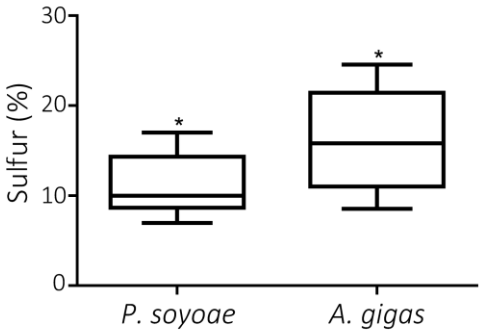

Figure 7 : Sulfur contents of vesicomyid gills. Data of sulfur content presented in the table are represented on the boxplot on the right.

4. Discussion

4.1. Structure of vesicomyid – symbiont communities at Guaymas Basin

Both morphological and molecular characterizations of vesicomyid species were performed to ascertain species identity, as previously recommended (Vrijenhoek et al., 1994; Peek et al., 1997; Goffredi et al., 2003; Audzijonyte et al., 2012; Decker et al., 2012). Three different vesicomyid species were identified at the studied sites. *Phreagena soyoae,* also known as *Phreagena kilmeri* (Peek et al., 1997; Kojima et al., 2004; Audzijonyte et al., 2012; Decker et al., 2012; Watanabe et al., 2013), *Calyptogena pacifica* and *Archivesica gigas* (Table 1). These results are consistent with previous taxonomical records from the Guaymas Basin (Simoneit et al., 1990; Peek et al., 1997; Ruelas-Inzunza et al., 2003; Soto, 2009). Species composition varied among sites. *P. soyoae* appeared predominant at both *Ayala* and *Vasconcelos* BIG5 sites (cold seep area) while *A. gigas* appeared predominant at the *Vasconcelos* BIG13 site (cold seep area) and was the only species detected at the hydrothermal vent area (*Morelos* site) (Table 1) (previously detected in other hydrothermal vent sediments at the Juan de Fuca ridge (Grehan and Juniper, 1996)). *C. pacifica,* was sampled only in small numbers at the cold seep sites and may be limited by depth (between 1 500 and 2 010 m, Table 1) as this species may be restricted to shallower depths (Goffredi et al., 2003; Krylova and Sahling, 2006; Krylova and Sahling, 2010; Decker et al., 2012). No *C. pacifica* was detected in the hydrothermal vent area, though some specimens of the species complex *C. pacifica / C. lepta* were previously reported from vents (Grassle et al., 1985; Simoneit et al., 1990). The latter samples were recently assigned to *C. lepta* (Audzijonyte et al., 2012). While no *C. lepta* was found during the "BIG" cruise, this species might be present at unsampled sites (*C. lepta* is rather small and more difficult to sample).

Either no (*A. gigas* and *P. soyoae*) or little (*C. pacifica*) *COI* intra-specific variation was detected. Although *A. gigas* is known to present genetic polymorphism (Osborn, 2001; Decker et al., 2012), individuals from hydrothermal vent and cold seep sites shared the same haplotype (Figure 4). This suggests a recent common history of the populations of the different species present at our sites, either through present day connectivity or through a recent common pool of ancestors having recently

394 colonized these sites. This low diversity might suggest drastic and potentially recurrent demographic
395 events.

396 Three different groups of bacterial symbionts, affiliated to the phylum *Gammaproteobacteria*,
397 were detected by our molecular analyses. Their presence and activity were confirmed by FISH
398 observations (Figures 4 and 5). Each vesicomyid species harbored one single specific symbiont and
399 symbiont lineages were highly similar among individuals of the same species, regardless of the site of
400 sampling. Furthermore, congruent phylogenetic topologies were obtained from the clam *COI* and
401 symbiont 16S rRNA, *aprA* and *cbbM* gene sequences (Figure 4). All these results support and confirm
402 a predominant vertical transmission in line with a co-evolution between vesicomyid species and their
403 associated symbiont lineages (e. g. Peek et al., 1998), independent of environmental influence (cold
404 seep or hydrothermal vent).

405 *4.2. Link between community composition and host biology and ecophysiology*

406 The diversity of the vesicomyid species and their distribution among and within the four
407 sampled environments might reflect differential niche preferences potentially linked to various life
408 characteristics for the vesicomyids, their symbionts, or both, as well as possible trophic or spatial
409 competition among the different species.

410 Possible ecophysiological differences between *P. soyoae* and *A. gigas* were suggested by our
411 observations and analyses. First, since all three vesicomyid species sampled in our study were found
412 indiscrimately in sediments where sulfide was detected or not (Table 1, Figure 3), we could not
413 explain the vesicomyid distribution in the Guaymas Basin on the basis of hydrogen sulfide
414 concentrations, as shown in other studies (Barry et al., 1997; Goffredi and Barry, 2002; Sahling et al.,
415 2002). Since vesicomyids symbionts require sulfide to live (Arp et al., 1984, Cavanaugh, 1983, Fiala-
416 Médioni and Métivier, 1986), these results could be due to our sampling strategy which used small
417 corers (5 cm in diameter) that could not collect sediments directly inside dense vesicomyid aggregates,
418 leading us to sample at the edges of vesicomyid aggregates. Moreover, we may have missed sulfide
419 increase at the *Ayala* site due to the short length of the core obtained (8 cm long) compared to other

sites where sulfide maximum was detected below this depth (Figure 3). However, these results revealed the high variability of sulfide concentrations and fluxes in vesicomyid habitats and pointed out the necessity of collecting sediments directly under vesicomyid clams as well as at the periphery of clam clusters. Nevertheless, when hydrogen sulfide and methane were detected in sediments, associated fluxes were comparable to values obtained in other cold seep areas where vesicomyids have been reported (DeBeer et al., 2006; Fischer et al., 2012), highlighting lower sulfide or methane fluxes or concentrations in vesicomyid beds than at microbial mats (Sahling et al., 2002; Levin et al., 2003).

Higher temperatures detected in the sediments of the *Morelos* hydrothermal vent site indicate harsher conditions for vesicomyid at Guaymas Basin vents than at seeps. Indeed, the positive increase in temperature with increasing depth in the sediments confirmed that the *Morelos* site is under hydrothermal influence; as was assumed to its proximity to the hydrothermal *MegaMat* site (about 240 m, Biddle et al, 2012, McKay et al., 2012). The hydrothermal influence could also shape other parameters not measured in our study (Von Damm et al., 1985; Kawka and Simoneit, 1987; Martens, 1990; De la Lanza-Espino and Soto, 1999). For example, heavy metals are usually present in hydrothermal fluids (Von Damm et al., 1985; Turnipseed et al., 2004) and are toxic in minute quantities if they are biologically available (Decho and Luoma, 1996). Higher levels of Cu were measured in the vesicomyid environment at the *Morelos* site, than at the *Vasconcelos* or the *Ayala* sites (Portail et al., 2015). Hydrothermal vent animals need detoxification mechanisms to deal with harmful effects of these toxic elements. Previous studies indicated that *A. gigas* could accumulate high concentrations of heavy metals with no signs of impairment (Ruelas-Inzunza et al., 2003). Therefore, the distribution of vesicomyid species in the Guaymas Basin might be due to a better tolerance of *A. gigas* compared to *P. soyoae* and *C. pacifica* to physico-chemical conditions potentially encountered in hydrothermally altered sediments of the Southern Trough area.

Traces of vesicomyid movements (Rosman et al., 1987; MacDonald et al., 1990) were visible on the soft sediments at the *Vasconcelos* BIG13 and the *Morelos* sites (Figure 2B and D), where *A. gigas* was dominant and sparsely distributed. No trace was observed at the *Ayala* and the *Vasconcelos* BIG5 sites where *P. soyoae* was dominant. Thus, a better ability to move might be a characteristic of *A.*

gigas. A softer and more liquid texture of sediments, as observed at the *Vasconcelos* BIG13 and *Morelos* sites (Table 1), might also favor vesicomyid locomotion. While no sulfide was detected at the *Vasconcelos* BIG13 site (or sulfide concentrations were under technical detection limit [10 µM]), high sulfide concentrations were measured at the BIG5 site (Table 1) and at the BIG18 microbial mat area, few meters apart (Vigneron et al., 2013). This might reveal a high spatial variability at the *Vasconcelos* sediments. Flux variations through time or at a small spatial scale could explain the lack of sulfide in the BIG13 sample. Reversal in flux directionality (switching between inflow and outflow conditions), could be a characteristic of vesicomyid habitats (Tryon and Brown, 2001; Levin et al., 2003). Therefore, thanks to its better ability to move, *A. gigas* could meet and exploit the transient and punctual sources of available sulfide, while they might remain unavailable to the less mobile *P. soyoae*. *A. gigas* could also exploit other sulfide-rich areas, such as microbial mats, and would manage to leave those areas where sulfide concentrations could be close to their toxic level (Vetter et al., 1991; Barry and Kochevar, 1998; Sahling et al., 2002). Thus, movements might be a response of the clam to variable fluid flows. However, proportions of species observed at each site seemed to indicate that as soon as global environmental conditions are suitable for the establishment of *P. soyoae*, *A. gigas* might be less competitive. However, where environmental resources have become depleted (such as at the *Vasconcelos* BIG13 site) or conditions are harsher (such as at the hydrothermal sediments), *A. gigas* would be more competitive, suggesting higher flexibility of this species.

4.3. Link between community composition and symbiont metabolisms

Consistently with previous studies of other vesicomyid species (Kuwahara et al., 2007; Newton et al., 2007), *cbbM* and *aprA* genes fragments were detected in all symbionts, confirming their potential autotrophic and thiotrophic metabolisms (Cavanaugh, 1983; Fiala-Médioni and Métivier, 1986; Goffredi and Barry, 2002).

In all our gill samples, white minerals identified as elemental sulfur were detected within the bacteriocyte zone (Figures 5A, 6A, B, C and D and Figure S1), no matter which storage method was used (stored directly at -80°C for the measurement of gill sulfur content, fixed for FISH for binocular

and SEM observations or storage of whole individual in ethanol 70% [data not shown]). These sulfur deposits might constitute inorganic energy reserves that would allow the symbiotic bacterial metabolism to function even during temporary absence of external sulfide supply, as previously suggested (Vetter, 1985; Fisher et al., 1988; Fiala-Médioni and Le pennec, 1989; Goffredi and Barry, 2002). The exclusive localization of these minerals in the bacteriocyte areas (Figure 6A) supported such a hypothesis. The unusual crystalline form observed in our samples could result from abiotic transformations of sulfur initially produced by symbionts, since a high reactivity of elemental sulfur, such as a fast recrystallization at room temperature, has already been observed (Hageage et al., 1970; Vetter, 1985; Pasteris et al., 2001; Goffredi and Barry, 2002). Very similar sulfur crystals have been detected in the siboglinid tubeworm *Sclerolinum contortum*, which inhabits hydrocarbon seeps (Eichinger et al., 2014). In that tubeworm, extracellular sulfur deposits were likely produced by the symbiotic bacteria and formation of these crystals was proposed to provide both energy-storage compounds for symbionts and a mechanism for removing excess toxic sulfide from host tissues (Eichinger et al., 2014). In our study, sulfur contents of *A. gigas* (16.1% of gill dry weight) were significantly higher than those of *P.soyoae* (11.3% of gill dry weight)(Figure 7). As previous studies showed a low level of sulfide oxidation products besides elemental sulfur in most of vesicomyid symbioses (Childress et al., 1991; Goffredi and Barry, 2002), our sulfur measurements probably reflect the elemental sulfur content. The difference observed between *A. gigas* and *P.soyoae* might be due to variations in sulfur storage and sulfide detoxification ability for each species. This difference could be explain by differences in the metabolic capabilities of the symbionts (potential for energy turnover and processing of sulfide) and/or vesicomyid species (sulfide uptake mechanism or sulfide-binding abilities)(Goffredi and Barry, 2002). This characteristic could allow *A. gigas* to live alternatively in low-sulfide and sulfide-rich areas, using stored sulfur in sulfide-depleted conditions. This hypothesis supports the assumption of clam movements, observed on the sediments, between areas depleted and enriched in sulfide and could explain the predominance of *A. gigas* at the *Vasconcelos* BIG13 site.

5. Conclusion

We performed the first analysis of vesicomyid distribution patterns at three cold seep and one hydrothermal vent sites in the Guaymas Basin. Distinct distributions of *A. gigas*, *P. soyoae* and *C. pacifica* were observed between sites with *A. gigas* being the dominant species in one seep site and in vent sediments while *P. soyoae* was the dominant species at two other seep sites. The same haplotype of *A. gigas* was found in both hydrothermal vent and cold seep areas, highlighting possible contemporary exchanges among neighboring and heavily sedimented seeps and vents within the Guaymas Basin. The diversity of the vesicomyid species and the heterogeneity in their distribution among and within the sampled environments may be explained by differences between host ecophysiological features and between the metabolic capabilities of their symbionts. The different sediment textures and the absence or presence of traces at some sites could indicate variability in vesicomyid behaviour. A better ability to move could allow *A. gigas* to easily meet and exploit transient and punctual sources of available sulfide. Moreover, the sulfur content in the gills of different vesicomyid species could indicate differences in host and/or associated symbiont metabolisms and highlight potential host and/or symbiont plasticity, which may allow *A. gigas* to colonize various environments. Host and associated symbionts might be able to adapt their metabolisms to environmental fluctuations. Future studies should further investigate bivalve behaviour as well as regulations of host and symbiont metabolisms, especially in the case of sulfur uptake and storage, in order to better understand bivalve distribution patterns in deep-sea chemosynthetic ecosystems.

Acknowledgements

We are indebted to the crews of the research vessel *L'Atalante* and the submersible *Nautile* of the cruise "BIG" and the scientific team for their work on board. This cruise was funded by IFREMER (France) and has benefited from a work permit in Mexican waters (DAPA/2/281009/3803, October 28 2009). We thank Lucile Durand, Richard Cosson and Priscilla Decottignies-Cognie for very helpful scientific discussions, Elena Krylova for her helpful comments on the morphological taxonomy and

the two anonymous reviewers for their comments on this manuscript. This study was supported by an IFREMER / Brittany region PhD grant to PC.

References

Altschul, S.F., Gish, W., Miller, W., Myers, E.W., and Lipman, D.J. (1990) Basic local alignment search tool. Journal of Molecular Biology 215: 403-410.

Amann, R.I., Binder, B.J., Olson, R.J., Chisholm, S.W., Devereux, R., and Stahl, D.A. (1990) Combination of 16S ribosomal-RNA-targeted oligonucleotide probes with flow-cytometry for analyzing mixed microbial populations. Applied and Environmental Microbiology 56: 1919-1925.

Arp, A.J., Childress, J.J., and Fisher, C.R. (1984) Metabolic and blood-gas transport characteristics of the hydrothermal vent bivalve Calyptogena magnifica. Physiological Zoology 57: 648-662.

Audzijonyte, A., Krylova, E.M., Sahling, H., and Vrijenhoek, R.C. (2012) Molecular taxonomy reveals broad trans-oceanic distributions and high species diversity of deep-sea clams (Bivalvia: Vesicomyidae: Pliocardiinae) in chemosynthetic environments. Systematics and Biodiversity 10: 403-415.

Barry, J.P., and Kochevar, R.E. (1998) A tale of two clams: differing chemosynthetic life styles among vesicomyids in Monterey Bay cold seeps. Cahiers De Biologie Marine 39: 329-331.

Barry, J.P., Kochevar, R.E., and Baxter, C.H. (1997) The influence of pore-water chemistry and physiology on the distribution of vesicomyid clams at cold seeps in Monterey Bay: Implications for patterns of chemosynthetic community organization. Limnology and Oceanography 42: 318-328.

Bennett, B.A., Smith, C.R., Glaser, B., and Maybaum, H.L. (1994) Faunal community structure of a chemoautotrophic assemblage on whale bones in the deep northeast Pacific Ocean. Marine Ecology-Progress Series 108: 205-205.

Biddle, J.F., Cardman, Z., Mendlovitz, H., Albert, D.B., Lloyd, K.G., Boetius, A., and Teske, A. (2012) Anaerobic oxidation of methane at different temperature regimes in Guaymas Basin hydrothermal sediments. Isme Journal 6: 1018-1031.

551 Boudreau, B.P. (1996) The diffusive tortuosity of fine-grained unlithified sediments. Geochimica et
552 Cosmochimica Acta 60: 3139-3142.
553 Cary, S., and Giovannoni, S. (1993) Transovarial inheritance of endosymbiotic bacteria in clams
554 inhabiting deep-sea hydrothermal vents and cold seeps. Proceedings of the National Academy of
555 Sciences of the United States of America 90: 5695 - 5699.
556 Cavanaugh, C.M. (1983) Symbiotic chemoautotrophic bacteria in marine-invertebrates from sulphid-
557 rich habitats. Nature 302: 58-61.
558 Childress, J., Fisher, C., Favuzzi, J., and Sanders, N. (1991) Sulfide and carbon dioxide uptake by the
559 hydrothermal vent clam, Calyptogena magnifica and its chemoautotrophic symbionts. Physiol Zool
560 64: 1444 - 1470.
561 Cruaud, P., Vigneron, A., Pignet, P., Caprais, J.-C., Lesongeur, F., Toffin, L. et al. (2015) Microbial
562 communities associated with benthic faunal assemblages at cold seep sediments of the Sonora Margin,
563 Guaymas Basin. Frontiers in Marine Science 2.
564 Cruaud, P., Vigneron, A., Pignet, P., Caprais, J.-C., Lesongeur, F., Toffin, L., et al. (2017).
565 Comparative Study of Guaymas Basin Microbiomes: Cold Seeps vs. Hydrothermal Vents Sediments.
566 Front. Mar. Sci. 4. doi:10.3389/fmars.2017.00417.
567 De la Lanza-Espino, G., and Soto, L.A. (1999) Sedimentary geochemistry of hydrothermal vents in
568 Guaymas Basin, Gulf of California, Mexico. Applied Geochemistry 14: 499-510.
569 DeBeer, D., Sauter, E., Niemann, H., Kaul, N., Foucher, J.P., and Witte, U. (2006) In situ fluxes and
570 zonation of microbial activity in surface sediments of the Haakon Mosby mud volcano. Limnol
571 Oceanogr 51: 1315-1331.
572 Decho, A.W., and Luoma, S.N. (1996) Flexible digestion strategies and trace metal assimilation in
573 marine bivalves. Limnology and Oceanography 41: 568-572.
574 Decker, C., Zorn, N., Le Bruchec, J., Caprais, J. C., Potier, N., Leize-Wagner, E., et al. (2017). Can
575 the hemoglobin characteristics of vesicomyid clam species influence their distribution in deep-sea
576 sulfide-rich sediments? A case study in the Angola Basin. Deep Sea Res. Part II Top. Stud. Oceanogr.
577 142, 219-232. doi:10.1016/j.dsr2.2016.11.009.

578 Decker, C., Zorn, N., Potier, N., Leize-Wagner, E., Lallier, F. H., Olu, K., et al. (2014). Globin's
579 Structure and Function in Vesicomyid Bivalves from the Gulf of Guinea Cold Seeps as an Adaptation
580 to Life in Reduced Sediments. Physiol. Biochem. Zool. 87, 855-869. doi:10.1086/678131.
581 Decker, C., Olu, K., Cunha, R.L., and Arnaud-Haond, S. (2012) Phylogeny and Diversification
582 Patterns among Vesicomyid Bivalves. Plos One 7.
583 Doyle, J.J. (1987) A rapid DNA isolation procedure for small quantities of fresh leaf tissue.
584 Phytochem Bull 19: 11-15.
585 Dubilier, N., Bergin, C., and Lott, C. (2008) Symbiotic diversity in marine animals: the art of
586 harnessing chemosynthesis. Nature Reviews Microbiology 6: 725-740.
587 Duperron, S., Nadalig, T., Caprais, J.C., Sibuet, M., Fiala-Medioni, A., Amann, R., and Dubilier, N.
588 (2005) Dual symbiosis in a Bathymodiolus sp mussel from a methane seep on the gabon continental
589 margin (southeast Atlantic): 16S rRNA phylogeny and distribution of the symbionts in gills. Applied
590 and Environmental Microbiology 71: 1694-1700.
591 Durand, L., Zbinden, M., Cueff-Gauchard, V., Duperron, S., Roussel, E.G., Shillito, B., and Cambon-
592 Bonavita, M.A. (2009) Microbial diversity associated with the hydrothermal shrimp Rimicaris
593 exoculata gut and occurrence of a resident microbial community. Fems Microbiology Ecology 71:
594 291-303.
595 Eichinger, I., Schmitz-Esser, S., Schmid, M., Fisher, C.R., and Bright, M. (2014) Symbiont-driven
596 sulfur crystal formation in a thiotrophic symbiosis from deep-sea hydrocarbon seeps. Environmental
597 Microbiology Reports 6: 364-372.
598 Endow, K., and Ohta, S. (1990) Occurrence of bacteria in the primary oocytes of vesicomyid clam
599 Calyptogena soyoae. Marine Ecology-Progress Series 64: 309-311.
600 Felsenstein, J. (1985) Confidence limits on phylogenies : an approach using the bootstrap. Evolution
601 39: 783-791.
602 Fiala-Médioni, A., and Métivier, C. (1986) Ultrastructure of the gill of the hydrothermal vent bivalve
603 Calyptogena magnifica, with a discussion of its nutrition. Marine Biology 90: 215-222.

Fiala-Médioni, A., and Lepennec, M. (1989) Adaptative features of the bivalve mollusks associated with fluid venting in the subduction zones off Japan. Palaeogeography Palaeoclimatology Palaeoecology 71: 161-167.

Fischer, D., Sahling, H., Nöthen, K., Bohrmann, G., Zabel, M., and Kasten, S. (2012) Interaction between hydrocarbon seepage, chemosynthetic communities, and bottom water redox at cold seeps of the Makran accretionary prism: insights from habitat-specific pore water sampling and modeling. Biogeosciences 9: 2013-2031.

Fisher, C. (1990) Chemoautotrophic and methanotrophic symbioses in marine invertebrates. Rev Aquat Sci 2: 399-436.

Fisher, C.R., Childress, J.J., Arp, A.J., Brooks, J.M., Distel, D.L., Dugan, J.A. et al. (1988) Variation in the hydrothermal vent clam, Calyptogen magnifica, at the Rose Garden vent on the Galapagos spreading center. Deep Sea Research Part A Oceanographic Research Papers 35: 1811-1831.

Folmer, O., Black, M., Hoeh, W., Lutz, R., and Vrijenhoek, R. (1994) DNA primers for amplification of mitochondrial cytochrome c oxidase subunit I from diverse metazoan invertebrates. Molecular Marine Biology and Biotechnology 3: 294-299.

Fonselius, S., Dyrssen, D., and Yhlen, B. (2007) Determination of hydrogen sulphide. In Methods of Seawater Analysis: Wiley-VCH Verlag GmbH, pp. 91-100.

Goffredi, S., Hurtado, L., Hallam, S., and Vrijenhoek, R. (2003) Evolutionary relationships of deep-sea vent and cold seep clams (Mollusca: Vesicomyidae) of the "pacifica/lepta" species complex. Marine Biology 142: 311 - 320.

Goffredi, S.K., and Barry, J.P. (2002) Species-specific variation in sulfide physiology between closely related Vesicomyid clams. Marine Ecology-Progress Series 225: 227-238.

Grassle, J., Brown-Leger, L., Morse-Porteous, L., Petrecca, R., and Williams, I. (1985) Deep-sea fauna of sediments in the vicinity of hydrothermal vents. Bulletin of the Biological Society of Washington: 443-452.

Grassle, J.F. (1986) The ecology of deep-sea hydrothermal vent communities. Advances in Marine Biology 23: 301-362.

631 Grehan, A.J., and Juniper, S.K. (1996) Clam distribution and subsurface hydrothermal processes at
632 Chowder Hill (Middle Valley), Juan de Fuca Ridge. Marine Ecology Progress Series 130: 105-115.
633 Hageage, G.J., Jr., Eanes, E.D., and Gherna, R.L. (1970) X-ray diffraction studies of the sulfur
634 globules accumulated by Chromatium species. Journal of Bacteriology 101: 464-469.
635 Iversen, N., and Jørgensen, B.B. (1993) Diffusion coefficients of sulfate and methane in marine
636 sediments: Influence of porosity. Geochimica et Cosmochimica Acta 57: 571-578.
637 Kato, S., Nakawake, M., Ohkuma, M., and Yamagishi, A. (2012) Distribution and phylogenetic
638 diversity of cbbM genes encoding RubisCO form II in a deep-sea hydrothermal field revealed by
639 newly designed PCR primers. Extremophiles 16: 277-283.
640 Katoh, K., Kuma, K.-i., Toh, H., and Miyata, T. (2005) MAFFT version 5: improvement in accuracy
641 of multiple sequence alignment. Nucleic Acids Research 33: 511-518.
642 Kawka, O.E., and Simoneit, B.R. (1987) Survey of hydrothermally-generated petroleums from the
643 Guaymas Basin spreading center. Organic geochemistry 11: 311-328.
644 Kimura, M. (1980) A simple method for estimating evolutionnary rates of base substitutions through
645 comparative studies of nucleotide sequences. Journal of Molecular Evolution 16: 111-120.
646 Kojima, S., Fujikura, K., and Okutani, T. (2004) Multiple trans-Pacific migrations of deep-sea
647 vent/seep-endemic bivalves in the family Vesicomyidae. Molecular Phylogenetics and Evolution 32:
648 396-406.
649 Kruskal, W.H., and Wallis, W.A. (1952) Use of ranks in one-criterion variance analysis. Journal of the
650 American statistical Association 47: 583-621.
651 Krylova, E.M., and Sahling, H. (2006) Recent bivalve molluscs of the genus Calyptogena
652 (Vesicomyidae). Journal of Molluscan Studies 72: 359-395.
653 Krylova, E.M., and Sahling, H. (2010) Vesicomyidae (Bivalvia): Current Taxonomy and Distribution.
654 Plos One 5.
655 Kuwahara, H., Yoshida, T., Takaki, Y., Shimamura, S., Nishi, S., Harada, M. et al. (2007) Reduced
656 genome of the thioautotrophic intracellular symbiont in a deep-sea clam, Calyptogena okutanii. Curr
657 Biol 17: 881 - 886.

Lazar, C.S., Parkes, R.J., Cragg, B.A., L'Haridon, S., and Toffin, L. (2012) Methanogenic activity and diversity in the centre of the Amsterdam Mud Volcano, Eastern Mediterranean Sea. Fems Microbiology Ecology 81: 243-254.

Levin, L.A., Ziebis, W., Mendoza, G.F., Growney, V.A., Tryon, M.D., Brown, K.M. et al. (2003) Spatial heterogeneity of macrofauna at northern California methane seeps: influence of sulfide concentration and fluid flow. Marine Ecology Progress Series 265: 123-139.

MacDonald, I.R., Guinasso, N., Jr., Reilly, J., Brooks, J., Callender, W.R., and Gabrielle, S. (1990) Gulf of Mexico hydrocarbon seep communities: VI. Patterns in community structure and habitat. Geo-Marine Letters 10: 244-252.

Mann, H.B., and Whitney, D.R. (1947) On a test of whether one of two random variables is stochastically larger than the other. The annals of mathematical statistics 18: 50-60.

Martens, C.S. (1990) Generation of short chain acid anions in hydrothermally altered sediments of the Guaymas Basin, Gulf of California. Applied Geochemistry 5: 71-76.

McKay, L.J., MacGregor, B.J., Biddle, J.F., Albert, D.B., Mendlovitz, H.P., Hoer, D.R. et al. (2012) Spatial heterogeneity and underlying geochemistry of phylogenetically diverse orange and white Beggiatoa mats in Guaymas Basin hydrothermal sediments. Deep Sea Research Part I: Oceanographic Research Papers 67: 21-31.

Meyer, B., and Kuever, J. (2007) Phylogeny of the alpha and beta subunits of the dissimilatory adenosine-5'-phosphosulfate (APS) reductase from sulfate-reducing prokaryotes - origin and evolution of the dissimilatory sulfate-reduction pathway. Microbiology-Sgm 153: 2026-2044.

Miller, M., Pfeiffer, W., and Schwartz, T. (2010) Creating the CIPRES Science Gateway for inference of large phylogenetic trees. 2010. In Proceedings of the Gateway Computing Environments Workshop (GCE) New Orleans, LA, USA, pp. 1-8.

Newton, I., Girguis, P., and Cavanaugh, C. (2008) Comparative genomics of vesicomyid clam (Bivalvia: Mollusca) chemosynthetic symbionts. Bmc Genomics 9: 585.

Newton, I., Woyke, T., Auchtung, T., Dilly, G., Dutton, R., Fisher, M. et al. (2007) The Calyptogena magnifica chemoautotrophic symbiont genome. Science 315: 998 - 1000.

685 Olu, K., Decker, C., Pastor, L., Caprais, J. C., Khripounoff, A., Morineaux, M., ... & Rabouille, C.
686 (2017). Cold-seep-like macrofaunal communities in organic-and sulfide-rich sediments of the Congo
687 deep-sea fan. Deep Sea Research Part II: Topical Studies in Oceanography, 142, 180-196.
688 Ondréas, H., Scalabrin, C., Fouquet, Y., & Godfroy, A. (2018). Recent high-resolution mapping of
689 Guaymas hydrothermal fields (Southern Trough) Cartographie haute résolution des champs
690 hydrothermaux de la ride sud du bassin de Guaymas. Bulletin de la Société Géologique de
691 France, 189(1).
692 Osborn, M. (2001) Molecular systematics of the vesicomyid clams: Calyptogena kilmeri and
693 Vesicomya gigas. MBARI report: 7.
694 Otero, X.L., Huerta-Diaz, M.A., and Mac??as, F. (2003) Influence of a turbidite deposit on the extent
695 of pyritization of iron, manganese and trace metals in sediments from the Guaymas Basin, Gulf of
696 California (Mexico). Applied Geochemistry 18: 1149-1163.
697 Pasteris, J.D., Freeman, J.J., Goffredi, S.K., and Buck, K.R. (2001) Raman spectroscopic and laser
698 scanning confocal microscopic analysis of sulfur in living sulfur-precipitating marine bacteria.
699 Chemical Geology 180: 3-18.
700 Paull, C.K., Ussler, W., III, Peltzer, E.T., Brewer, P.G., Keaten, R., Mitts, P.J. et al. (2007) Authigenic
701 carbon entombed in methane-soaked sediments from the northeastern transform margin of the
702 Guaymas Basin, Gulf of California. Deep-Sea Research Part Ii-Topical Studies in Oceanography 54:
703 1240-1267.
704 Peek, A.S., Gustafson, R.G., Lutz, R.A., and Vrijenhoek, R.C. (1997) Evolutionary relationships of
705 deep-sea hydrothermal vent and cold-water seep clams (Bivalvia: Vesicomyidae): results from the
706 mitochondrial cytochrome oxidase subunit I. Marine Biology 130: 151-161.
707 Peek, A.S., Feldman, R.A., Lutz, R.A., and Vrijenhoek, R.C. (1998) Cospeciation of
708 chemoautotrophic bacteria and deep sea clams. Proceedings of the National Academy of Sciences of
709 the United States of America 95: 9962-9966.
710 Portail, M., Olu, K., Escobar-Briones, E., Caprais, J.C., Menot, L., Waeles, M. et al. (2015)
711 Comparative study of vent and seep macrofaunal communities in the Guaymas Basin. Biogeosciences
712 12: 5455-5479.

713 Rosman, I., Boland, G.S., and Baker, J.S. (1987) Epifaunal aggregations of Vesicomyidae on the
714 continental slope off Louisiana. Deep Sea Research Part A Oceanographic Research Papers 34: 1811-
715 1820.
716 Ruelas-Inzunza, J., Soto, L.A., and Páez-Osuna, F. (2003) Heavy-metal accumulation in the
717 hydrothermal vent clam Vesicomya gigas from Guaymas basin, Gulf of California. Deep Sea Research
718 Part I: Oceanographic Research Papers 50: 757-761.
719 Sahling, H., Rickert, D., Lee, R.W., Linke, P., and Suess, E. (2002) Macrofaunal community structure
720 and sulfide flux at gas hydrate deposits from the Cascadia convergent margin, NE Pacific. Marine
721 Ecology-Progress Series 231: 121-138.
722 Saitou, N., and Nei, M. (1987) The Neighbor-Joining Method - a New Method for Reconstructing
723 Phylogenetic Trees. Molecular Biology and Evolution 4: 406-425.
724 Sarradin, P.-M., and Caprais, J.-C. (1996) Analysis of dissolved gases by headspace sampling gas
725 chromatography with column and detector switching. Preliminary results. Analytical Communications
726 33: 371-373.
727 Sarradin, P.-M., Waeles, M., Bernagout, S., Le Gall, C., Sarrazin, J., and Riso, R. (2009) Speciation of
728 dissolved copper within an active hydrothermal edifice on the Lucky Strike vent field (MAR, 37°N).
729 Science of The Total Environment 407: 869-878.
730 Sibuet, M., and Olu, K. (1998) Biogeography, biodiversity and fluid dependence of deep-sea cold-seep
731 communities at active and passive margins. Deep-Sea Research Part Ii-Topical Studies in
732 Oceanography 45: 517-+.
733 Simoneit, B.R.T., Lonsdale, P.F., Edmond, J.M., and Shanks, W.C. (1990) Deep-Water Hydrocarbon
734 Seeps in Guaymas Basin, Gulf of California. Applied Geochemistry 5: 41-49.
735 Soto, L.A. (2009) Stable carbon and nitrogen isotopic signatures of fauna associated with the deep-sea
736 hydrothermal vent system of Guaymas Basin, Gulf of California. Deep-Sea Research Part Ii-Topical
737 Studies in Oceanography 56: 1675-1682.
738 Stamatakis, A. (2006) RAxML-VI-HPC: maximum likelihood-based phylogenetic analyses with
739 thousands of taxa and mixed models. Bioinformatics 22: 2688-2690.

740 Stewart, F. (2008) Genetic diversification and evolution of chemosynthetic endosymbionts in deep-sea
741 clams (Vesicomyidae). (Doctoral dissertation, Harvard University).
742 Stewart, F., Newton, I., and Cavanaugh, C. (2005) Chemosynthetic endosymbioses: adaptations to
743 oxic-anoxic interfaces. Trends Microbiol 13: 439 - 448.
744 Tamura, K., Dudley, J., Nei, M., and Kumar, S. (2007) MEGA4: Molecular Evolutionary Genetics
745 Analysis (MEGA) software version 4.0. Molecular Biology and Evolution 24: 1596-1599.
746 Teske, A., Hinrichs, K.U., Edgcomb, V., Gomez, A.D., Kysela, D., Sylva, S.P. et al. (2002) Microbial
747 diversity of hydrothermal sediments in the Guaymas Basin: Evidence for anaerobic methanotrophic
748 communities. Applied and Environmental Microbiology 68: 1994-2007.
749 Tryon, M.D., and Brown, K.M. (2001) Complex flow patterns through Hydrate Ridge and their impact
750 on seep biota. Geophysical Research Letters 28: 2863-2866.
751 Tunnicliffe, V. (1991) The biology of hydrothermal vents - Ecology and Evolution. Oceanography and
752 Marine Biology 29: 319-407.
753 Turnipseed, M., Jenkins, C.D., and Van Dover, C.L. (2004) Community structure in Florida
754 Escarpment seep and Snake Pit (Mid-Atlantic Ridge) vent mussel beds. Marine Biology 145: 121-132.
755 Van Dover, C.L., German, C.R., Speer, K.G., Parson, L.M., and Vrijenhoek, R.C. (2002) Evolution
756 and Biogeography of Deep-Sea Vent and Seep Invertebrates. Science 295: 1253-1257.
757 Vetter, R.D. (1985) Elemental sulfur in the gills of three species of clams containing
758 chemoautotrophic symbiotic bacteria: a possible inorganic energy storage compound. Marine Biology
759 88: 33-42.
760 Vetter, R.D., Powell, M.A., and Somero, G.N. (1991) Metazoan adaptations to hydrogen sulphide.
761 Metazoan life without oxygen (Bl)'ant, C; editor) Chapman and Ha/I: 109-128.
762 Vigneron, A., Cruaud, P., Pignet, P., Caprais, J.-C., Cambon-Bonavita, M.-A., Godfroy, A., and
763 Toffin, L. (2013) Archaeal and anaerobic methane oxidizer communities in the Sonora Margin cold
764 seeps, Guaymas Basin (Gulf of California). The ISME journal 7: 1595-1608.
765 Von Damm, K.L., Edmond, J.M., Measures, C.I., and Grant, B. (1985) Chemistry of submarine
766 hydrothermal solutions at Guaymas Basin, Gulf of California. Geochimica Et Cosmochimica Acta 49:
767 2221-2237.

Vrijenhoek, R.C., Schutz, S.J., Gustafson, R.G., and Lutz, R.A. (1994) Cryptic species of deep-sea clams (Mollusca: Bivalvia: Vesicomyidae) from hydrothermal vent and cold-water seep environments. Deep Sea Research Part I: Oceanographic Research Papers 41: 1171-1189.

Watanabe, H., Seo, E., Takahashi, Y., Yoshida, T., Kojima, S., Fujikura, K., and Miyake, H. (2013) Spatial distribution of sister species of vesicomyid bivalves Calyptogena okutanii and Calyptogena soyoae along an environmental gradient in chemosynthetic biological communities in Japan. Journal of Oceanography 69: 129-134.

Wilcoxon, F. (1945) Individual comparisons by ranking methods. Biometrics bulletin 1: 80-83.

Zhou, J., Bruns, M., and Tiedje, J. (1996) DNA recovery from soils of diverse composition. Appl Environ Microbiol 62: 316-322.

Figure S1 : Observations and EDX spectra of the white minerals observed at the abfrontal zone of vesicomyid gill filaments. (A) Image of gill abfrontal zone fixed for FISH (binocular microscope), showing the white minerals. (B) Sample of minerals isolated by dissection and observed with SEM. (C), (D), (E) and (F) Spectra and composition of (C) negative control on aluminum background, (D) the mineral on aluminum background as negative control, (E) copper background as negative control and (F) the mineral on copper background.

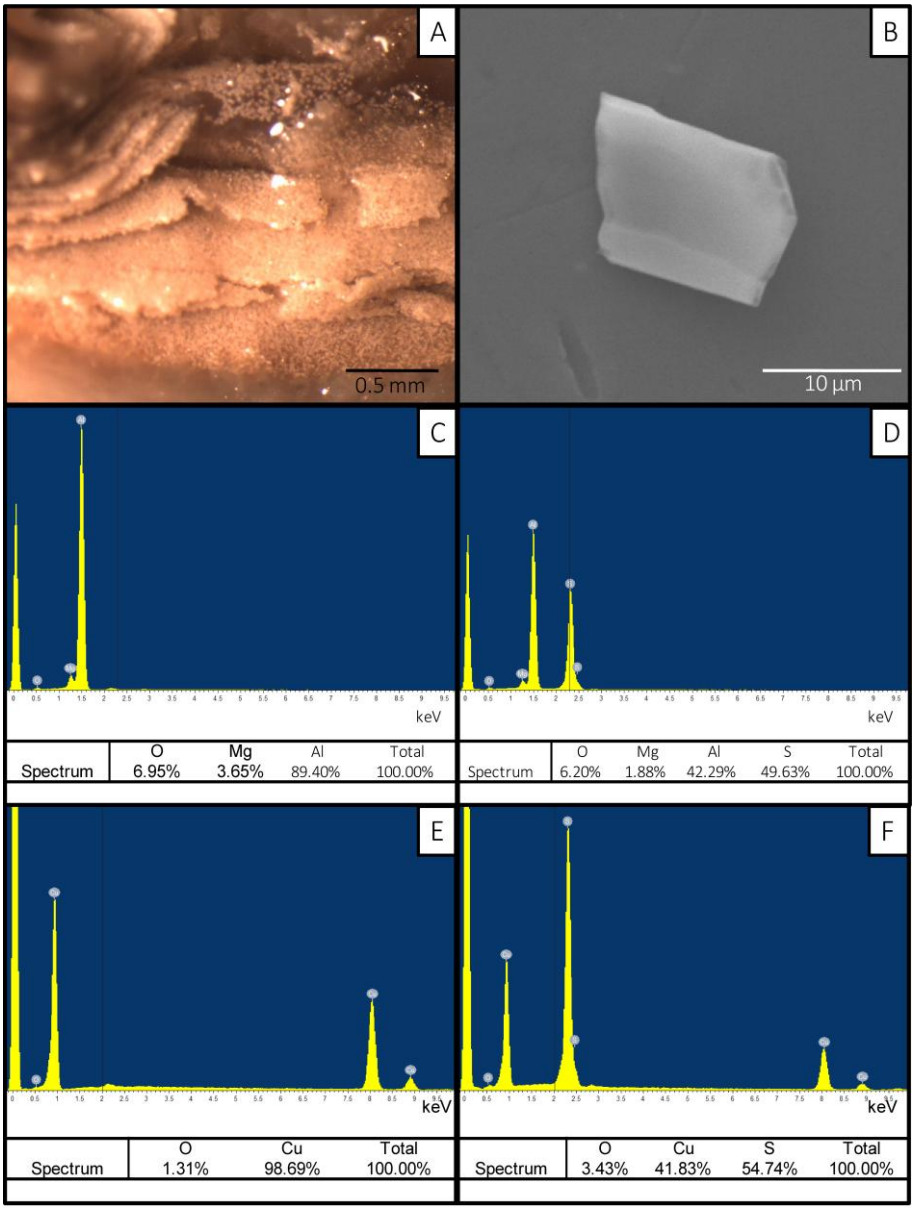

788 **Table S1 :** Primers used for PCR and oligonucleotide probes used for fluorescence *in situ*

789 hybridization.

Name	*Function*	*Target gene*	*Sequence (5' - 3')*	*Annealing temp. (°C) (PCR)*	*% formamide (FISH)*
LCO1490 HCO2198	PCR	*COI (universal)*	GGT-CAA-CAA-ATC-ATA-AAG-ATA-TTG-G TAA-ACT-TCA-GGG-TGA-CCA-AAA-AAT-CA	60	
VesLCO VesHCO	PCR	*COI (Vesicomyid specific)*	TTA-ATA-GGA-ACT-GCT-TTT-AG TCA-CCC-AAA-CCA-GCA-GGA-TC	60	
E338F 1407R	PCR	*16S rRNA (Bacteria)*	ACT-CCT-ACG-GGA-GGC-AGC GAC-GGG-CGG-TGW-GTR-CAA	54	/
AprA-1-FW AprA-5-RV	PCR	*APS reductase*	TGG-CAG-ATC-ATG-ATY-MAY-GG GCG-CCA-ACY-GGR-CCR-TA	58	
cbbm343F cbbm1226R	PCR	*RuBP oxygenase/carboxylase Form II*	GGY-AAY-AAC-CAR-GGY-ATG-GG CGY-ARB-GCR-TTC-ATR-CCR-CC	50	
Eub338	FISH	*16S rRNA Bacteria*	GCT-GCC-TCC-CGT-AGG-AGT	/	35
Psoyoae	FISH	*16S rRNA P. soyoae symbionts*	GTA-CCC-CCC-CCA-ACG-GCT		35
Agigas	FISH	*16S rRNA A. gigas symbionts*	GTA-ACC-CCC-CCA-ACG-GCT		35
Cpacifica	FISH	*16S rRNA C. pacifica symbionts*	GTA-ACC-CCC-TCA-ACG-ACT		35

Abbreviations: COI, cytochrome c oxidase I ; APS reductase, adenosine-5'-phosphosulfate reductase; RuBP, ribulose-1, 5- biphosphate.

790